The TFIIH components p44/p62 act as a damage sensor during nucleotide excision repair

Barnett JT[1], Kuper J[2], Koelmel W[2], Kisker C[2] and Kad NM[1,*]

1 School of Biological Sciences, University of Kent, Canterbury, CT2 7NH, United Kingdom.

2 Rudolf Virchow Center for Experimental Biomedicine, Institute for Structural Biology, University of Würzburg, 97080 Würzburg, Germany.

[*] To whom correspondence may be addressed. Email: n.kad@kent.ac.uk

Keywords; DNA repair, NER, fluorescence imaging, single molecule

Abstract

Nucleotide excision repair (NER) protects the genome following exposure to diverse types of DNA damage, including UV light and chemotherapeutics. Mutations in human NER genes lead to diseases such as xeroderma pigmentosum and Cockayne syndrome [1]. In eukaryotes, the major transcription factor TFIIH is the central hub of NER. The core components of TFIIH include the helicases XPB, XPD, and the five core 'structural' subunits [2-6]. Two of these core-TFIIH proteins, p44 and p62 remain relatively unstudied; although p44 is known to regulate the helicase activity of XPD during NER [7-9]. p62's role is thought to be structural [10]; however, a recent cryo-EM structure [11] shows p44, p62, and XPD making contacts with each other, implying a more extensive role in DNA repair beyond the structural integrity of TFIIH. Here, we show that p44 stimulates XPD's ATPase, but upon encountering DNA damage further stimulation is only observed when p62 is in the ternary complex. More significantly, we show that the p44/p62 complex binds DNA independently of XPD and diffuses along its backbone, indicating a novel DNA-binding entity in TFIIH. These data support a role for p44/p62 in TFIIH's mechanism of damage detection. This revises our understanding of TFIIH and prompts more extensive investigation of all of the core subunits, for an active role during both DNA repair and transcription.

Results and Discussion

XPD's ATPase is stimulated by p44/p62

p44 contacts both p62 and XPD in TFIIH [3,11,12], and mutations in XPD that disrupt p44 or p62 binding cause defects in NER and result in disease[3,7,8,12]. To investigate if p44/p62 was able to stimulate the ATPase of XPD, the turnover of ATP in the presence of different DNA substrates was measured using an NADH-coupled assay.

In the absence of p44 and p62, XPD's ATPase activity is slow even in the presence of single-stranded DNA (0.043 s^{-1}). However, with a p44 fragment (residues 1-285 (N-p44)) containing the von Willebrand domain, XPD's ATPase was significantly stimulated in the presence of both double- and single-stranded DNA[8] (~0.03 s^{-1} to 0.136 s^{-1} and 0.504 s^{-1} respectively $p < 0.05$ (**Figure 1**)). No further acceleration of the ATPase was observed with full length p44 co-expressed in complex with p62 (p44/p62). However, remarkably, when damage (a fluorescein moiety shown to proxy for damage [13]) was introduced into a dsDNA substrate, p44/p62 accelerated XPD's ATPase two-fold more than on undamaged DNA (**Figure 1A & B**). N-p44 alone could not accelerate XPD's ATPase in the presence of damage, indicating the ternary complex (p44/p62) is responsible for this further enhancement and thus may play an important role in lesion detection. These results may explain why truncations of the yeast p62 homologue (Tfb1) sensitize the organism to UV irradiation [14-16].

To further investigate the role of p44 and p62 in activating XPD we analyzed XPD's helicase activity on an open fork substrate. Again, p44/p62 is seen to play an active role by enhancing the helicase activity compared to N-p44 alone (**Figure 1C**). Although no damage is present in the open fork substrate, p44/p62 significantly enhances XPD's ability to successfully unwind the DNA substrate

(two-fold more than XPD with N-p44), despite no change in ATPase activity (**Figure 1A**).

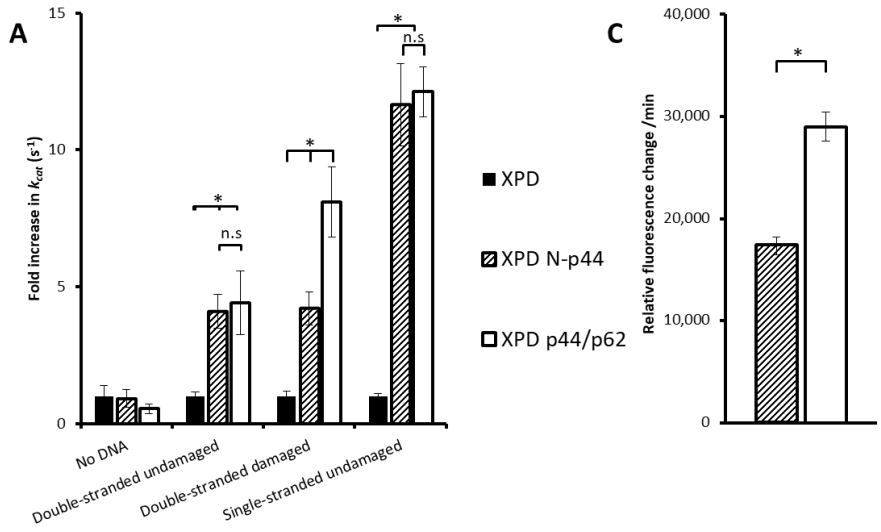

B

DNA substrate	XPD k_{cat} values (s^{-1}) alone, with N-p44, and p44/p62		
	XPD	XPD N-p44	XPD p44/p62
No DNA	0.046 ± 0.013	0.042 ± 0.008	0.025 ± 0.004
Double-stranded undamaged	0.033 ± 0.004	0.136 ± 0.013	0.146 ± 0.035
Double-stranded damaged	0.027 ± 0.004	0.114 ± 0.006	0.218 ± 0.019
Single-stranded undamaged	0.043 ± 0.003	0.504 ± 0.055	0.524 ± 0.016

Figure 1. Steady-state ATPase and helicase activity of XPD in the presence of various DNA substrates and core TFIIH proteins*. A) The activity of XPD's ATPase is stimulated by both N-p44 (dashed) and p44/p62 (white) on various DNA substrates. Values for k_{cat} are given as a fold change from XPD alone (black). Errors are shown as S.E.M from 3 repeats. B) Table showing k_{cat} values ± S.E.M for XPD's ATPase. C) XPD's helicase activity is stimulated by N-p44 (dashed) and p44/p62 (white) on an open fork substrate. XPD alone displays no helicase activity [8]. Errors are shown as S.E.M from 9 repeats. Statistical*

*significance determined using a student's t-test where * = $p < 0.05$, n.s = not statistically significant.*

The p44/p62 complex directly binds DNA

The role of p44/p62 in the recognition of damage presents the intriguing possibility that this complex could interact with DNA independently from XPD. To investigate this, we used a single molecule DNA tightrope assay [17] (**Figure 2**). Conjugation of a fluorescent quantum dot (QDot) to the poly-histidine purification tag on the p44/p62 complex [18] was achieved using an anti-His IgG antibody. Substantial binding of p44/p62 to dsDNA was observed, and of these approximately 80% could diffuse (n = 599 total) providing the first direct evidence that these TFIIH subunits are able to bind DNA independently of XPD.

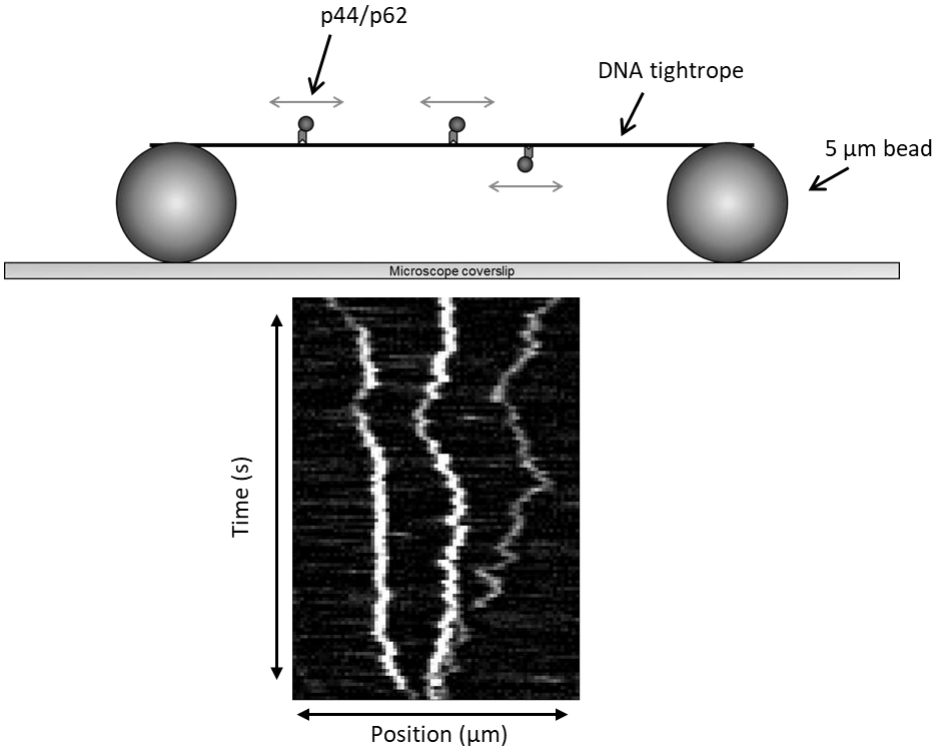

Figure 2. Schematic of a tightrope and kymograph analysis. *DNA tightropes are formed between beads adhered to a coverslip. QDot labelled proteins are then observed binding to the DNA. A video can be transformed into a kymograph by plotting position through time. Diffusing molecules appear as movement in the X axis for a duration of frames (Y axis). The kymograph shown in the lower panel indicates three diffusing p44/p62 molecules.*

The p44/p62 complex displayed multiple types of behavior on DNA. Firstly, we observed complexes randomly diffusing along the DNA, unable to pass one another (**Figure 2**). Secondly while diffusing, pausing was seen, often at the same location on the tightropes. This may indicate a visit to a damage site or a specific sequence. Finally, fluorescence intensity fluctuations of the same molecule over time suggest possible oligomerization. At elevated salt concentrations (100 mM vs 10 mM KCl) fewer molecules bound to DNA, and of these, a lower percentage diffused (55%, n = 58 total). We calculated the diffusion constant using mean-squared displacement analysis [17] and found no significant change ($p > 0.05$) between salt conditions (10 mM KCl 0.067 $\mu m^2/s$ $\pm$ 0.006 vs 100 mM KCl 0.042 $\mu m^2/s$ $\pm$ 0.010), which suggests that p44/p62 molecules slide along the DNA helix [19]. Based on the estimated size of a p44/p62 complex conjugated to a QDot, the diffusion constant appears limited by rotation-coupled diffusion around the backbone of the DNA helix [20]. This is consistent with the inability for complexes to pass one another on the DNA.

In summary, we present the first mechanistic characterisation of the non-helicase TFIIH subunits p44/p62. Complexes formed by these two proteins were observed to bind and slide on dsDNA. Our bulk phase ATPase and helicase data indicate that p44/p62 is involved in damage recognition. One could speculate that p44/p62 actively enhances TFIIH activity towards scanning the opened repair bubble to position TFIIH factors for subsequent excision.

Nonetheless, our results clearly show that the p44/p62 complex plays an active and not just a structural role in the TFIIH complex.

Methods

Purification

The genes encoding p44 and p62 were cloned from *C. thermophilum* cDNA. p62 was cloned into the pETM-11 vector (EMBL) without a tag. p44 was cloned into the pBADM-11 vector (EMBL) containing an N-terminal hexa-Histidine tag followed by a TEV cleavage site. p62 and p44 were co-expressed in *E. coli* BL21 CodonPlus (DE3) RIL cells (Agilent) and were co-purified via immobilized metal affinity chromatography (Ni TED, Machery-Nagel), followed by size exclusion chromatography (SEC), and anion exchange chromatography (AEC). SEC was conducted with a HiLoad 16/600 Superdex 200 prep grade column (GE Healthcare) in 20 mM Hepes pH 7.5, 250 mM NaCl, and 1 mM TCEP. AEC was conducted with a MonoQ 5/50 GL column (GE Healthcare). The proteins were eluted via a salt gradient ranging from 50 to 1000 mM NaCl. AEC buffers were composed of 20 mM HEPES pH 7.5, 50/1000 mM NaCl, and 1 mM TCEP. The p62/p44 protein complex was concentrated to approximately 20 mg/ml and flash frozen in liquid nitrogen for storage.

XPD and N-p44 (1-285) from *C. thermophilum* were cloned as described previously [21]. XPD was expressed as N-terminally His-tagged proteins in *E. coli* ArcticExpress (DE3)-RIL cells (Agilent). Cells were grown in TB medium at 37°C until they reached an OD_{600} of 0.6-0.8. Expression was started with the addition of 0.05% L-arabinose and performed at 11°C for 20 h. p44 was expressed as N-terminally His-tagged protein in *E. coli* BL21-CodonPlus (DE3)-RIL cells (Stratagene). Cells were grown as described for ctXPD and

expression was started by adding 0.1 mM IPTG at 14°C for 18 h. XPD and p44 were purified to homogeneity by metal affinity chromatography (Ni-IDA, Macherey&Nagel) as described previously [21] followed by size exclusion chromatography (SEC) (20 mM HEPES pH 7.5, 200 mM NaCl) and an additional anion exchange chromatography (AEC) step in the case of XPD. AEC was performed using a MonoQ 5/50 GL column (GE Healthcare) with 20 mM HEPES pH 7.5, 50 mM NaCl, and 1 mM TCEP as loading buffer and the same buffer containing 1 M NaCl was used for elution. The final buffer after AEC was 20 mM HEPES pH 7.5, 250 mM NaCl, and 1 mM TCEP. The proteins were concentrated to at least 5 mg/ml based on their calculated extinction coefficient using ProtParam (SwissProt) and then flash frozen for storage at -80°C.

ATPase assay

dsDNA substrates used:

F26,50 contains a fluorescein moiety covalently attached to thymine (*);

5`GACTACGTACTGTTACGGCTCCATCT*CTACCGCAATCAGGCCAGA TCTGC 3`

The reverse complementary sequence to F26,50;

5`GCAGATCTGGCCTGATTGCGGTAGCGATGGAGCCGTAACAGTACG TAGTC 3`

F26,50 without the fluorescein moiety;

5`GACTACGTACTGTTACGGCTCCATCTCTACCGCAATCAGGCCAGAT CTGC 3`

The NADH-coupled ATPase assay was performed as described previously [22] in plate reader format. Imaging buffer containing the NADH-reaction components was supplemented with 1 mM fresh TCEP, protein (100 nM (equimolar concentrations for XPD N-p44 and XPD p44/p62)), and 50 nM of DNA substrate. The reaction was started with the addition of 1 mM ATP to each well, and the change in OD340 (NADH) was monitored every 8 seconds/well over 30

minutes at room temperature in a Clariostar plate reader. The rates of NADH consumption were used to calculate k_{cat}. Reactions were repeated 3 times, and S.E.M used as errors values.

In vitro helicase assay

Helicase activity was analyzed utilizing a fluorescence-based helicase assay. We used an open fork substrate with a Cy3 label at the 3' end of the translocated strand where unwinding of the DNA substrate reduces quenching of the Cy3 fluorescence.
5`AGCTACCATGCCTGCACGAATTAAGCAATTCGTAATCATGGTCATA GC-Cy3 3` and a dabcyl modification on the 5' end of the opposite strand
5` Dabcyl-
GCTATGACCATGATTACGAATTGCTTGGAATCCTGACGAACTGTAG 3`
Assays were carried out in 20 mM HEPES pH 7.5, 50 mM KCl, 5 mM $MgCl_2$, and 1 mM TCEP. DNA was used at a concentration of 250 nM. Helicase activity was measured with equimolar concentrations of XPD, p44, and/or p62. The mix of reagents, with the exception of ATP, were preincubated at 37°C and the reaction was subsequently started with the addition of 5 mM ATP. Kinetics were recorded with a Flourostar Optima plate reader (BMG labtech). Fluorescence was detected at an excitation wavelength of 550 nm (slit width, 2 nm) and an emission wavelength of 570 nm (slit width, 2 nm). Initial velocities were fitted with the MARS software package (BMG labtech) and represent the averages of at least three different reactions and two independent protein batches.

Single Molecule DNA Tightrope Assay

For a detailed protocol see [18]. p44/p62 interactions with DNA were studied in imaging buffer (20 mM Tris pH 8.0, 10 mM KCl (100 mM for high salt), 5 mM

200 $MgCl_2$, 1 mM TCEP). Videos for diffusion analysis were collected between 30
201 seconds and 5 minutes at 10 frames per second. Video analysis was performed
202 in ImageJ as described previously [17].
203

204 ## Acknowledgements

205 We would like to thank the members of the Kad group for useful discussions.
206 This work was supported by the Biotechnology and Biological Sciences
207 Research Council BB/P00847X/1, BB/M019144/1, BB/I003460/1 to NMK and
208 BB/M01603X/1 to JTB and by the German Research Foundation KI-562/7-1 to
209 CK. The authors declare no conflict of interest.
210

211 ## Author contributions

212 Collected data: JTB, JK, WK. Designed experiments: JTB, JK, CK, NMK.
213 Analysed Data: JTB, JK, NMK. Wrote paper: JTB, JK, CK, NMK.
214

215 ## References

216

217 1 Compe, E. & Egly, J. M. TFIIH: when transcription met DNA repair. *Nat*
218 *Rev Mol Cell Biol* **13**, 343-354, doi:10.1038/nrm3350 (2012).
219 2 Roy, R. *et al.* The DNA-dependent ATPase activity associated with the
220 class II basic transcription factor BTF2/TFIIH. *J Biol Chem* **269**, 9826-
221 9832 (1994).
222 3 Luo, J. *et al.* Architecture of the Human and Yeast General Transcription
223 and DNA Repair Factor TFIIH. *Mol Cell* **59**, 794-806,
224 doi:10.1016/j.molcel.2015.07.016 (2015).
225 4 Araujo, S. J. *et al.* Nucleotide excision repair of DNA with recombinant
226 human proteins: definition of the minimal set of factors, active forms of
227 TFIIH, and modulation by CAK. *Genes Dev* **14**, 349-359 (2000).
228 5 Svejstrup, J. Q. *et al.* Different forms of TFIIH for transcription and DNA
229 repair: holo-TFIIH and a nucleotide excision repairosome. *Cell* **80**, 21-28
230 (1995).
231 6 Sung, P. *et al.* Human xeroderma pigmentosum group D gene encodes a
232 DMA helicase. *Nature* **365**, 852-855, doi:10.1038/365852a0 (1993).

7 Coin, F. *et al.* Mutations in the XPD helicase gene result in XP and TTD phenotypes, preventing interaction between XPD and the p44 subunit of TFIIH. *Nature Genetics* **20**, 184-188, doi:Doi 10.1038/2491 (1998).

8 Kuper, J. *et al.* In TFIIH, XPD helicase is exclusively devoted to DNA repair. *PLoS biology* **12**, e1001954 (2014).

9 Coin, F., Oksenych, V. & Egly, J. M. Distinct roles for the XPB/p52 and XPD/p44 subcomplexes of TFIIH in damaged DNA opening during nucleotide excision repair. *Mol Cell* **26**, 245-256, doi:10.1016/j.molcel.2007.03.009 (2007).

10 Liu, H. *et al.* Structure of the DNA repair helicase XPD. *Cell* **133**, 801-812, doi:10.1016/j.cell.2008.04.029 (2008).

11 Greber, B. J., Toso, D. B., Fang, J. & Nogales, E. The complete structure of the human TFIIH core complex. *Elife* **8**, doi:10.7554/eLife.44771 (2019).

12 Bernardes de Jesus, B. M., Bjoras, M., Coin, F. & Egly, J. M. Dissection of the molecular defects caused by pathogenic mutations in the DNA repair factor XPC. *Mol Cell Biol* **28**, 7225-7235, doi:10.1128/MCB.00781-08 (2008).

13 Buechner, C. N. *et al.* Strand-specific recognition of DNA damages by XPD provides insights into nucleotide excision repair substrate versatility. *J Biol Chem* **289**, 3613-3624, doi:10.1074/jbc.M113.523001 (2014).

14 Gervais, V. *et al.* TFIIH contains a PH domain involved in DNA nucleotide excision repair. *Nat Struct Mol Biol* **11**, 616-622, doi:10.1038/nsmb782 (2004).

15 Gileadi, O., Feaver, W. J. & Kornberg, R. D. Cloning of a subunit of yeast RNA polymerase II transcription factor b and CTD kinase. *Science* **257**, 1389 (1992).

16 Matsui, P., DePaulo, J. & Buratowski, S. An interaction between the Tfb1 and Ssl1 subunits of yeast TFIIH correlates with DNA repair activity. *Nucleic Acids Research* **23**, 767-772 (1995).

17 Kad, N. M., Wang, H., Kennedy, G. G., Warshaw, D. M. & Van Houten, B. Collaborative dynamic DNA scanning by nucleotide excision repair proteins investigated by single- molecule imaging of quantum-dot-labeled proteins. *Mol Cell* **37**, 702-713, doi:10.1016/j.molcel.2010.02.003 (2010).

18 Springall, L., Inchingolo, A. V. & Kad, N. M. DNA-Protein Interactions Studied Directly Using Single Molecule Fluorescence Imaging of Quantum Dot Tagged Proteins Moving on DNA Tightropes. *Methods Mol Biol* **1431**, 141-150, doi:10.1007/978-1-4939-3631-1_11 (2016).

19 von Hippel, P. H. & Berg, O. G. Facilitated target location in biological systems. *J Biol Chem* **264**, 675-678 (1989).

20 Schurr, J. M. The one-dimensional diffusion coefficient of proteins absorbed on DNA. *Biophysical Chemistry* **9**, 413-414, doi:10.1016/0301-4622(75)80057-3 (1979).

21 Kuper, J. *et al.* In TFIIH, XPD Helicase Is Exclusively Devoted to DNA Repair. *Plos Biology* **12**, doi:ARTN e1001954 10.1371/journal.pbio.1001954 (2014).

22 Barnett, J. T. & Kad, N. M. Understanding the coupling between DNA damage detection and UvrA's ATPase using bulk and single molecule kinetics. *FASEB journal* **33**, 763-769, doi:10.1096/fj.201800899R (2019).